



Shape coexistence in ^{186}Pb : beyond-mean-field description by configuration mixing of symmetry restored wave functions

T. Duguet^{a,1}, M. Bender^{b,*}, P. Bonche^a, P.-H. Heenen^b

^a *Service de Physique Théorique, CEA Saclay, 91191 Gif-sur-Yvette cedex, France*

^b *Service de Physique Nucléaire Théorique, Université Libre de Bruxelles, C.P. 229, B-1050 Bruxelles, Belgium*

Received 27 January 2003; received in revised form 28 February 2003; accepted 3 March 2003

Editor: W. Haxton

Abstract

We study shape coexistence in ^{186}Pb using configuration mixing of angular-momentum and particle-number projected self-consistent mean-field states. The same Skyrme interaction SLy6 is used everywhere in connection with a density-dependent, zero-range pairing force. The model predicts coexisting spherical, prolate and oblate 0^+ states at low energy.

© 2003 Published by Elsevier Science B.V. Open access under [CC BY license](http://creativecommons.org/licenses/by/3.0/).

PACS: 21.10.Dr; 21.10.Pc; 21.60.Jz

The behavior of shell effects away from the valley of stability is a topic of very active investigation, both theoretically and experimentally. For light nuclei, the spherical $N = 20$ and $N = 28$ shells disappear in neutron-rich isotopes, leading to strongly deformed ground states and large $B(E2)$ transition probabilities between the first 2^+ state and the ground state [1]. In contrast, the magic proton number $Z = 82$ is particularly strong and its influence persists even in very neutron-deficient nuclei. The ground state of Pb isotopes is known to be spherical down to ^{182}Pb [2]. The weakening of the magicity of the $Z = 82$ shell manifests itself through the appearance of low-lying 0^+ states [3]. At least one low-lying, excited 0^+

level has been observed in all even–even Pb isotopes between $A = 182$ and 194 at excitation energies below 1 MeV, the most extreme cases being ^{188}Pb and ^{186}Pb [4,5] with two excited 0^+ states below 700 keV.

Two different kinds of models have been invoked to explain the coexistence of several 0^+ states at low energy [6]. In a shell model picture [5], the first excited 0^+ level observed from ^{202}Pb down to ^{186}Pb is interpreted as a two-quasiparticle proton configuration $(\pi h_{9/2})^2$, while the second one in ^{188}Pb and ^{186}Pb as well as the first 0^+ state in ^{184}Pb are understood as a four-quasiparticle configuration $(\pi h_{9/2})^4$. In this picture, neutrons and protons outside the inert core interact through pairing and quadrupole interactions to generate deformed structures. Such a model requires a drastic truncation of the configuration space. Up to now, it has only been applied in rather schematic and qualitative ways.

* Corresponding author.

E-mail address: mbender@ulb.ac.be (M. Bender).

¹ Current address: Physics Division, Argonne National Laboratory, Argonne, IL 60439, USA.

In mean-field models, the 0^+ states observed at low energies are associated with coexisting energy minima which appear for different values of the axial quadrupole moment [7]. The ground state corresponds to the spherical minimum and the excited 0^+ level to a deformed state with an oblate (in the heaviest Pb isotopes) or a prolate (in ^{184}Pb up to ^{188}Pb) shape.

However, shape coexistence in the neutron-deficient Pb region cannot be described on the level of mean-field models in a fully satisfactory way. The minima obtained as a function of the quadrupole moment are rather shallow and dynamical effects such as quadrupole vibrations may affect the very existence of these minima. Tajima et al. [8] and, more recently, Chasman et al. [9] have studied the quadrupole dynamics of Pb isotopes by performing a configuration mixing of mean-field states with different axial quadrupole moments. Their results support the interpretation of the excited 0^+ states as deformed minima. The lowest excited levels obtained in the configuration mixing calculation have average deformations close to that of the mean-field minima. However, the calculated excitation energies overestimate the experimental values. Diabatic effects have been studied by Tajima et al. who have included, for each axial quadrupole moment, the lowest Hartree–Fock+BCS (HFBCS) configuration and the two-quasiparticle deformed proton configurations $(\pi h_{9/2})^2$. Tajima et al. have shown that these configurations do not influence the configuration-mixing results significantly, and that they can be neglected.

The experimental data on neutron deficient Pb isotopes are not limited to a few 0^+ states. Rotational bands have also been observed whose properties have served to interpret the excited 0^+ state as associated with oblate and prolate deformations. Transition probabilities between the levels are also known in some cases. It seems, therefore, highly desirable to apply the configuration-mixing method that we have recently developed [10] to Pb isotopes. This method treats simultaneously the most important symmetry restorations and the mixing with respect to a collective variable. Here, we present an application to ^{186}Pb . This isotope has the unique property of having 0^+ levels as its lowest three states, with the excitation energy of the second and third 0^+ also being the lowest among the known Pb isotopes [5]. While the ground state is assumed to be spherical, the 0^+ states observed at

532 keV and 650 keV are interpreted as corresponding to oblate and prolate configurations.

The “projected” configuration mixing of mean-field wave functions performed here has several goals. The particle-number projection removes unwanted contributions coming from states with different particle numbers, which are an artifact of the BCS approach. The angular momentum projection separates the contribution from different angular momenta to the mean-field states and generates wave functions in the laboratory frame with good angular momentum. Finally, the variational configuration mixing with respect to a collective coordinate, the axial quadrupole moment in this work, removes the contributions to the ground state coming from collective vibrations, and simultaneously provides the excitation spectrum corresponding to this mode.

The starting point of our method is a set of independent HFBCS wave functions $|q\rangle$ generated by mean-field calculations with a constraint on a collective coordinate q . Such mean-field states break several symmetries of the exact many-body states. Wave functions with good angular momentum and particle numbers are obtained by the restoration of rotational and particle-number symmetry on $|q\rangle$:

$$|JMq\rangle = \frac{1}{\mathcal{N}} \sum_K g_K^J \hat{P}_{MK}^J \hat{P}_Z \hat{P}_N |q\rangle, \quad (1)$$

where \mathcal{N} is a normalization factor. \hat{P}_{MK}^J , \hat{P}_N , \hat{P}_Z are projectors onto the angular momentum J with projection M along the laboratory z -axis, neutron number N and proton number Z , respectively. We impose axial symmetry and time reversal invariance and, therefore, K can only be 0 and we shall omit the coefficient $g_K^J = \delta_{K0}$. This prescription excludes the description of γ bands where $K = 2$.

A variational configuration mixing on the collective variable q is then performed for each angular momentum

$$|JMk\rangle = \sum_q f_k^{JM}(q) |JMq\rangle. \quad (2)$$

The weight functions $f_k^{JM}(q)$ are determined by requiring that the expectation value of the energy

$$E_k^{JM} = \frac{\langle JMk | \hat{H} | JMk \rangle}{\langle JMk | JMk \rangle} \quad (3)$$

is stationary with respect to an arbitrary variation $\delta f_k^{JM}(q)$. This prescription leads to the discretized Hill–Wheeler equation [11]. Such a secular problem amounts to a restricted variation after projection in the set of states obtained for different values of the collective variable q . Collective wave functions in the basis of the intrinsic states are then obtained from the set of weight functions $f_k^{JM}(q)$ by a basis transformation [8]. In $|JMk\rangle$, the weight of each mean-field state $|q\rangle$ is given by:

$$g_k^{JM}(q) = \langle JMk|q\rangle. \quad (4)$$

Since the collective states $|JMk\rangle$ have good angular momentum, quadrupole moments and transition probabilities can be determined directly in the laboratory frame of reference without further approximations.

The same effective interaction is used to generate the mean-field wave functions and to perform the configuration mixing calculation. We have chosen the Skyrme interaction SLy6 in the mean-field channel [12] and a density-dependent, zero-range force as defined in [13], in the pairing channel. The pairing equations are solved using the Lipkin–Nogami prescription, as done in [10]. The two-body center-of-mass correction is self-consistently included in the interaction SLy6 [12]. However, in the present calculations, it is included *a posteriori* at the mean-field level as well as in the projection and configuration-mixing calculations.

In Fig. 1 the deformation energy of ^{186}Pb is plotted before and after projection on angular momentum. All curves are drawn versus the intrinsic axial quadrupole moment of the unprojected mean-field states. As projected $J = 0$ states are spherical, this “quadrupole moment” is only a convenient way to label the projected states. The curve labeled “mean-field” plots the deformation energy after particle-number projection only. It exhibits a spherical global minimum as well as local minima at prolate and oblate deformations. While the deformation energy of the prolate minimum fortuitously reproduces the experimental value of 0.650 MeV for the prolate 0^+ state, the 1.1 MeV deformation energy of the oblate minimum overestimates the experimental value of 0.532 MeV for the oblate 0^+ level. A fourth, very shallow, minimum can be seen at a deformation $\beta_2 \approx 0.5$; it is too shallow to be safely associated with a physical state.

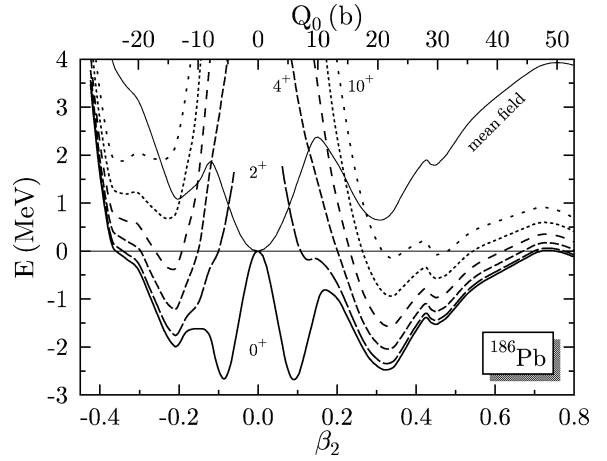


Fig. 1. Particle-number projected (“mean field”) and particle-number and angular-momentum projected potential energy curves up to $J = 10$ for ^{186}Pb as a function of the mass quadrupole moment in barn (upper axis) or, equivalently, in terms of β_2 (lower axis). The energy reference is that of the projected spherical mean-field state.

The energy curves obtained after angular momentum projection are also shown in Fig. 1. At moderate deformations, around the prolate and oblate minima, the mean-field states are dominated by angular momentum components with $J \geq 8$. This is reflected in the fact that all projected energy curves are far below the mean-field one. The spherical mean-field state is rotationally invariant and, therefore, contributes to $J = 0$ only. Two minima appear at small deformations, around $\beta_2 = \pm 0.1$. They do not correspond to two different states, but to the correlated spherical state (see below). For larger prolate and oblate deformations, the energy difference between the mean-field and $J = 0$ curves stays nearly constant. The prolate and oblate mean-field minima are present in all the projected energy curves. Angular momentum projection reduces the energy difference between the spherical ($|\beta_2| \approx 0.1$) and deformed minima to 0.2 MeV for the prolate and 0.68 MeV for the oblate well. While the prolate potential well is pronounced for all angular momenta, the oblate one now becomes very shallow for $J = 0$.

The excitation energies E_k^{JM} of the collective states $|JMk\rangle$ obtained from the configuration mixing calculation are shown in Fig. 2. Each of these states is represented by a horizontal bar drawn at the average intrinsic deformation $\sum_q \beta_2(q) |g_k^{JM}(q)|^2$, where $\beta_2(q)$ is

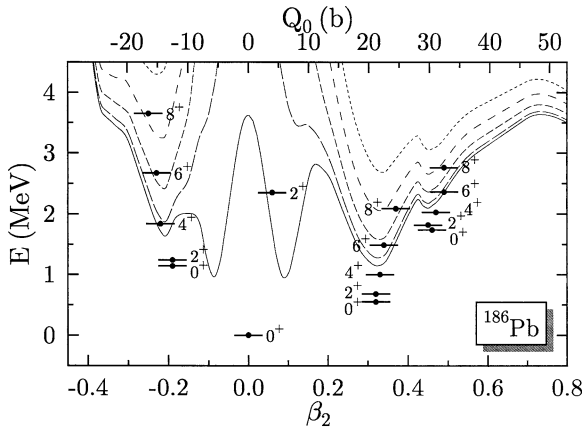


Fig. 2. Spectrum of the lowest positive parity bands with even angular momentum and $K = 0$, as a function of the deformation (see text). The angular momentum projected energy curves are shown for comparison. The energy reference is that of the calculated 0_1^+ ground state.

the deformation of the mean-field state. The excitation spectrum is divided into bands associated with different deformations. Configuration mixing lowers the energy of the lowest collective states with respect to the projected energy curves. The energy gain is the largest for the ground state, hence increasing the excitation energies of the prolate and oblate 0^+ levels.

The corresponding collective wave functions $g_k^{JM}(q)$ are presented in Fig. 3. Their square gives the weight of each mean-field state $|q\rangle$ in the collective state $|JMk\rangle$.

The ground state wave function is spread in a similar way on both oblate and prolate sides with a zero value for the average β_2 deformation. The wave functions of the first two excited 0^+ states are strongly peaked at either prolate (0_2^+) or oblate deformation (0_3^+), with their tails extending into the spherical well. For higher J values, the shape of the wave functions confirms their assignment to oblate and prolate bands, as already hinted so in Fig. 2. As there is no spherical well for $J > 0$ states, their wave functions mix only prolate and oblate configurations. Starting with $J = 4$, all levels are strongly localized and are predominantly either prolate or oblate. The shapes of the 0_4^+ , 2_3^+ , and 4_3^+ wave functions suggest their interpretation as a rotational band built on a β vibration within the prolate well, while the wave function of the 2_4^+ state indicates

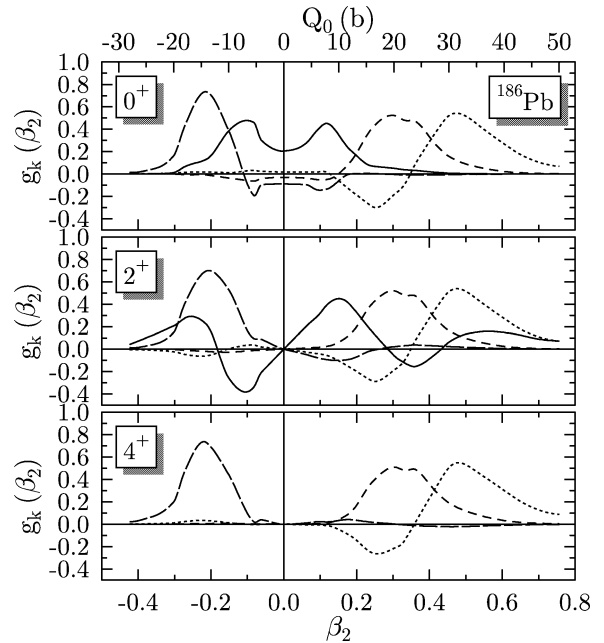


Fig. 3. GCM wave functions of the lowest $|JMk\rangle$ states. Solid lines denote spherical states, long-dashed lines the oblate band, dashed lines the prolate band, and dotted lines the β band in the prolate well.

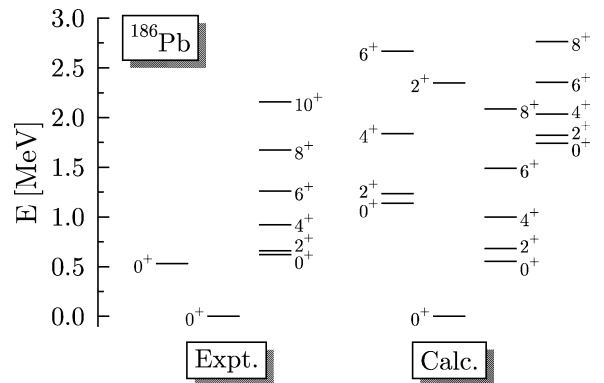


Fig. 4. Comparison between the calculated excitation energies and the available experimental data for low-lying states in ^{186}Pb . From the left to the right the spectra show oblate, spherical and prolate bands.

that it corresponds to a vibrational state, which is spread over the entire potential well.

The calculated spectrum is compared with the experimental data in Fig. 4. The excitation energy of the prolate 0^+ state at 0.55 MeV is very close to the experimental value. In contrast, the excitation

energy of the oblate 0^+ level is largely overestimated. The experimental data even suggest that the oblate state is slightly below the prolate one. A nice result from the calculations is that the structure of the first three 0^+ levels is dominated by spherical, prolate and oblate configurations, respectively, and this supports the interpretation of the experimental data in terms of shape coexistence. This feature could not have been guessed from the deformation energy curves (see Fig. 1), where the oblate well has a depth of only 500 keV in contrast with the prolate one of 1 MeV. The excitation energies of the first two excited 0^+ states are even quite close to the energy differences between the deformed minima and the spherical minimum of the mean-field deformation energy curve.

Both experimentally and theoretically, all bands exhibit a rotational behavior, with the exception of the $E_{0^+} - E_{2^+}$ energy difference which is too small. This can be understood from the stronger state mixing for the $J = 0$ than for higher J values which is observed in the calculations. For the prolate band, however, the displacement from a rotational behavior remains too small. This is probably a consequence of the overestimated energy of the oblate band head which reduces the mixing between the deformed configurations.

Calculated transition probabilities for $J > 2$ states confirm the separation of the excited states into rotational bands with very small $B(E2)$ transitions between them. While the transition quadrupole moments, Q_0 , of the oblate ($Q_0 \approx -600 e \text{ fm}^2$ or $\beta_2 \approx -0.2$) and prolate ($Q_0 \approx 1000 e \text{ fm}^2$ or $\beta_2 \approx 0.34$) bands slowly grow with angular momentum, the deformation of the third rotational band stays nearly constant at about $Q_0 \approx 1400 e \text{ fm}^2$ ($\beta_2 \approx 0.49$), in agreement with the systematics of the minima in the projected energy curves of Fig. 1. The $B(E2)$ values for the in and out of band $2^+ \rightarrow 0^+$ transitions confirm that the low-lying 0^+ states are indeed mixed.

Our results strongly support the interpretation of the Pb isotopes spectra as evidence for shape coexistence. There remains, however, a significant overestimation of one of the band's excitation energy. This could be due to several ingredients of the model:

- The effective mean-field interaction; small differences between interactions (surface tension, spin-orbit strength, ...) shift the relative energies of

the various coexisting minima at the mean-field level [14,15]. In a calculation with the Skyrme SLy4 interaction, the prolate and oblate 0^+ states are pushed up to 1.05 MeV and 1.39 MeV, respectively, as can be expected from the overall stiffer energy surface of this interaction [16].

- The strength and the form factor of the pairing interaction; a test with a reduced pairing strength (-1100 MeV fm^3) shows that the energies of the prolate and oblate minima of the deformation energy curves are reduced to 0.2 MeV and 0.65 MeV, respectively.
- The configuration space used in the configuration mixing; to test this possible source of error, we have enlarged the space by including the oblate $(\pi h_9/2)^2$ two-quasiparticle proton configurations, as was done by Tajima et al. [8]. As in this work, the results are changed by at most 100 keV.
- The inclusion of triaxial quadrupole configurations; projection on J becomes much heavier numerically, and this is still beyond present numerical possibilities.
- Generalized interaction for calculations beyond mean field; most mean-field interactions depend on the one-body density. It is known since the 70s that this density dependence can have two different origins: either a three-body force or a resummation of (short-range) correlations. To generalize this dependence for the non-diagonal matrix elements appearing beyond the mean-field approximation, we have chosen the generalisation stemming from a three-body interaction. Resummation of correlations beyond mean-field gives rise to another generalisation of the Skyrme force [17]. The study of shape coexistence in nuclei like the Pb isotopes could be a good place to determine the merits of both generalisations of the Skyrme force.

Acknowledgements

This research was supported in part by the PAI-P5-07 of the Belgian Office for Scientific Policy. We thank M. Huyse, R. Janssens and P. Van Duppen for fruitful and inspiring discussions. M.B. acknowledges support through a European Community Marie Curie Fellowship.

References

- [1] P.-G. Reinhard, D.J. Dean, W. Nazarewicz, J. Dobaczewski, J.A. Maruhn, M.R. Strayer, *Phys. Rev. C* 60 (1999) 014316.
- [2] J. Wauters, N. Bijmens, H. Folger, M. Huyse, H.Y. Hwang, R. Kirchner, J. von Schwarzenberg, P. Van Duppen, *Phys. Rev. C* 50 (1994) 2768.
- [3] R. Julin, K. Helariutta, M. Muikki, *J. Phys. G* 27 (2001) R109.
- [4] J. Heese, K.H. Maier, H. Grawe, J. Grebosz, H. Klüge, W. Meczynski, M. Schramm, R. Schubart, K. Spohr, J. Styczen, *Phys. Lett. B* 302 (1993) 390.
- [5] A.N. Andreyev, M. Huyse, P. Van Duppen, L. Weissman, D. Ackermann, J. Gerl, F. Heßberger, S. Hofmann, A. Kleinbohl, G. Münzenberg, S. Reshitko, C. Schlegel, H. Schaffner, P. Cagarda, M. Matos, S. Saro, A. Keenan, C. Moore, C.D. O’Leary, R.D. Page, M. Taylor, H. Kettunen, M. Leino, A. Lavrentiev, R. Wyss, K. Heyde, *Nature* 405 (2000) 430.
- [6] J.L. Wood, K. Heyde, W. Nazarewicz, M. Huyse, P. Van Duppen, *Phys. Rep.* 215 (1992) 101.
- [7] W. Nazarewicz, *Phys. Lett. B* 305 (1993) 195.
- [8] N. Tajima, H. Flocard, P. Bonche, J. Dobaczewski, P.-H. Heenen, *Nucl. Phys. A* 551 (1993) 409.
- [9] R.R. Chasman, J.L. Egidio, L.M. Robledo, *Phys. Lett. B* 513 (2001) 325.
- [10] A. Valor, P.-H. Heenen, P. Bonche, *Nucl. Phys. A* 671 (2001) 145.
- [11] D.L. Hill, J.A. Wheeler, *Phys. Rev.* 89 (1953) 1102.
- [12] E. Chabanat, P. Bonche, P. Haensel, J. Meyer, R. Schaeffer, *Nucl. Phys. A* 635 (1998) 231.
- [13] C. Rigollet, P. Bonche, H. Flocard, P.-H. Heenen, *Phys. Rev. C* 59 (1999) 3120.
- [14] M. Bender, T. Cornelius, G.A. Lalazissis, J.A. Maruhn, W. Nazarewicz, P.-G. Reinhard, *Eur. Phys. J. A* 14 (2002) 23.
- [15] T. Niksic, D. Vretenar, P. Ring, G.A. Lalazissis, *Phys. Rev. C* 65 (2002) 054320.
- [16] M. Bender, K. Rutz, P.-G. Reinhard, J.A. Maruhn, *Eur. Phys. J. A* 7 (2000) 467.
- [17] T. Duguet, P. Bonche, Density dependence of two-body interactions for beyond mean-field calculations, *Phys. Rev. C*, in press, nucl-th/0210057.